

DATAR: DEFORMABLE AUDIO TRANSFORMER FOR AUDIO EVENT RECOGNITION

Wentao Zhu

Address - Line 1
Address - Line 2
Address - Line 3

ABSTRACT

Transformers have achieved promising results on a variety of tasks. However, the quadratic complexity in self-attention computation has limited the applications, especially in low-resource settings and mobile or edge devices. Existing works have proposed to exploit hand-crafted attention patterns to reduce computation complexity. However, such hand-crafted patterns are data-agnostic and may not be optimal. Hence, it is likely that relevant keys or values are being reduced, while less important ones are still preserved. Based on this key insight, we propose a novel deformable audio Transformer for audio recognition, named DATAR, where a deformable attention equipping with a pyramid transformer backbone is constructed and learnable. Such an architecture has been proven effective in prediction tasks, *e.g.*, event classification. Moreover, we identify that the deformable attention map computation may over-simplify the input feature, which can be further enhanced. Hence, we introduce a learnable input adaptor to alleviate this issue, and DATAR achieves state-of-the-art performance.

Index Terms— Deformable Audio Transformer, Audio Adaptor, Event Classification

1. INTRODUCTION

Transformer [1] is firstly introduced to address natural language processing tasks, *e.g.*, machine translation. Recently, it has shown great potential in the field of audio and speech recognition [2, 3, 4]. Transformer-based models, *i.e.*, self-attention, are good at modeling long-range dependencies, which are proven to achieve superior performance in the regime of a large amount of learnable model parameters and training data. However, the quadratic computational complexity of the Transformer to the number of input tokens limits the applications, especially in low-resource settings. Specifically, the superfluous number of keys to attend per query yields high computational costs and slow convergence.

To address the issue of excessive attention computation, [5, 6, 7, 8] have leveraged carefully designed efficient attention patterns to alleviate the computation complexity. However, since the hand-crafted attention patterns are data-agnostic and may not be optimal, it probably leads to that relevant keys or

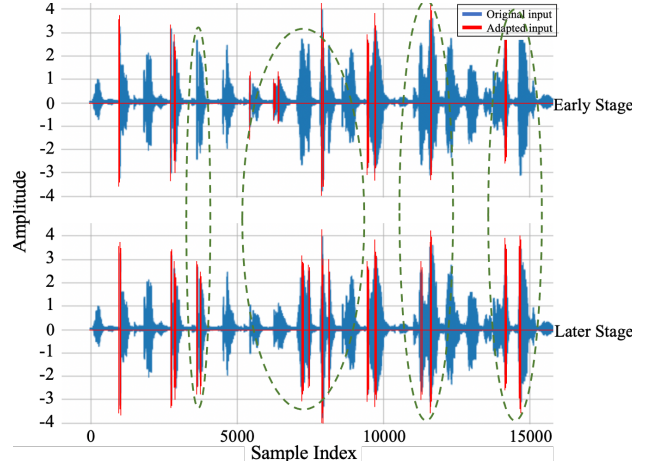


Fig. 1. Visualization of the effectiveness of proposed learnable input adaptor, which enhances relatively important parts of the original signal, a log-compressed mel-scaled spectrogram, to become more distinguishable, colored by green dash ovals.

values being dropped, while less important ones are still preserved. To tackle the issue of hand-crafted attention patterns, [9] exploits an efficient deformable attention to generate the candidate key or value set for a given query flexibly. Moreover, the mechanism makes the model be able to adapt to each individual input. Recently, deformable attention-based networks have yielded promising results on many challenging tasks [10, 11, 12]. Hence, this motivates us to explore the deformable attention mechanism in audio transformers.

In this work, a deformable audio transformer, DATAR, is proposed in Fig. 2. DATAR is equipped with a powerful pyramid backbone based on the deformable attention. Such a backbone is popular in prediction tasks, *e.g.*, image classification [12]. Based on the observation in [13, 14], global attention typically results in almost the same attention patterns for various queries. Hence, a trainable audio offset generator (AOG) is introduced to learn a few groups of query-agnostic offsets to shift keys and values to important regions. Such a design not only helps hold a linear space complexity, but also introduces a deformable attention pattern to transformer backbones. Specifically, for each self-attention module, reference

points are first generated as uniform grids, which are the same across the input data. Then, the introduced AOG takes input as the query features and generates the corresponding offsets for all the reference points. Hence, the candidates of keys or values are shifted towards important regions. This augments the self-attention module with higher efficiency and flexibility to capture more informative features.

Furthermore, we identify that the training of DATAR faces an accuracy improvement bottleneck, which is most likely due to that the deformable attention map calculation oversimplifies the input feature, leading to information loss [12]. We address this challenge by introducing a learnable input adaptor that adds learnable signals to the original input for more accurate deformable audio attention map computation. As these learned signals make the important parts of the original input become more distinguishable, the effectiveness of deformable audio attention is improved in Fig. 1.

2. RELATED WORK

Transformers [1] have been validated in the fields of natural language processing and computer vision. Recently, [15, 16, 4] introduce the Transformer into audio and speech processing and achieve the state-of-the-art performance. AST [15] proposes a convolution-free audio spectrogram Transformer, which is directly applied to an audio spectrogram and capable of capturing long-range global context even in the lowest layers. However, it requires large GPU memory and long training time, which limits the model’s scalability in audio related tasks [16]. MAST and HTS-AT [17, 16, 18, 19] introduce a hierarchical structure into the AST for audio event detection. Inspired by the two pathways in the human auditory system, [4] introduces a two-stream ConvNet for audio recognition, *i.e.*, fusing slow and fast streams with multi-level lateral connections. The slow pathway has a higher channel capacity, while the fast pathway has fewer channels and operates at a fine-grained temporal resolution. Different from the AST, [20, 3, 2] combine the Transformer architecture and ConvNet for audio processing. [20, 3] stack a Transformer on top of a ConvNet. [2] combines a Transformer and a ConvNet in each model block. Other efforts combine ConvNets with simpler attention modules [21, 22, 23]. The main model structure of DATAR is convolution-free.

The main challenge of self-attention is the quadratic computation complexity [1, 24]. [25, 26, 7, 27, 8, 28, 29] have proposed various efficient methods to address this issue. The improvements focus on learning multiscale features for prediction tasks or efficient attention mechanisms. These efficient attention mechanisms include global tokens [25, 30, 31], windowed attention [26, 7], dynamic token sizes [32], and focal attention [28]. Deformable convolution [9, 33] is a powerful technique to attend to flexible locations conditioned on input data. Recently, [10, 34, 35] have applied it to vision Transformers (ViT). Deformable DETR [10] improves the con-

vergence speed of DETR [36] by selecting a few keys for each query on the top of a ConvNet backbone. [34, 35] introduce deformable modules to refine visual tokens. [34] introduces a spatial sampling module before a ViT backbone to improve visual tokens. [35] proposes to refine patches across stages by deformable patch embeddings. We are the first to exploit deformable attention in audio event classification.

3. METHODOLOGY

The main idea of deformable attention is to flexibly generate discriminative key and value points for each query token, compared with a regular grid sampling strategy in a conventional Transformer. This learned deformable sampling strategy yields a more useful and discriminative dot-product matrix and output. To ease the computational complexity of deformation generation, we leverage the redundancy in the signal, and the offset network is conducted in $4\times$ subsampled tokens by a convolutional neural network followed by bilinear interpolation.

3.1. Deformable Audio Transformer

Let $X \in \mathbb{R}^{h \times T}$ be an audio spectrogram as input for DATAR, where h is the number of triangular mel-frequency bins, and T is the temporal length. After the patch embedding, which can be a convolutional block conducted in the audio spectrogram, we obtain the embedding token matrix $A \in \mathbb{R}^{N \times C}$, where C is the embedding dimension and N is the number of tokens. A multi-head self-attention (MHSA) block with M heads is formulated:

$$\begin{aligned} q &= AW_q, \quad k = AW_k, \quad v = AW_v, \\ z^{(m)} &= \sigma(q^{(m)} k^{(m)\top} / \sqrt{d}) v^{(m)}, \quad m = 1, \dots, M, \\ z &= \text{Concat} \left(z^{(1)}, \dots, z^{(M)} \right) W_o, \end{aligned}$$

where $\sigma(\cdot)$ denotes the softmax function, and $d = C/M$ is the dimension of each head. $z^{(m)}$ denotes the embedding output from the m -th attention head, $q^{(m)}, k^{(m)}, v^{(m)} \in \mathbb{R}^{N \times d}$ denote query, key, and value embeddings respectively. $W_q, W_k, W_v, W_o \in \mathbb{R}^{C \times C}$ are the projection matrices. To build up a Transformer block, an MLP block with two linear layers and a GELU activation is usually adopted to provide nonlinearity. With layer normalization [37] (LN) and identity shortcuts, the l -th Transformer block is formulated as:

$$\begin{aligned} z'_l &= \text{MHSA}(\text{LN}(z_{l-1})) + z_{l-1}, \\ z_l &= \text{MLP}(\text{LN}(z'_l)) + z'_l. \end{aligned} \quad (1)$$

Deformable attention module Given the input feature map $X \in \mathbb{R}^{h \times T}$, we generate a uniform grid of points $p \in \mathbb{R}^{h_G \times T_G \times 2}$ as the references in Fig. 2. Specifically, the grid size is down-sampled from the input feature map size by a factor r , $h_G = h/r$, $T_G = T/r$. The values of reference points are linearly spaced 2D coordinates

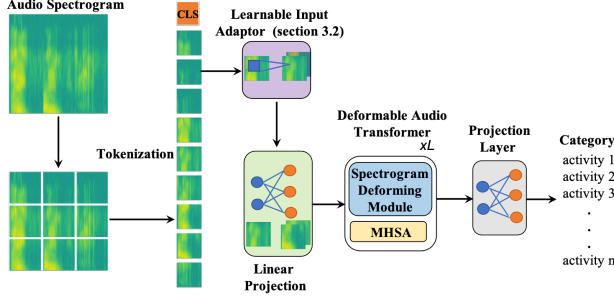


Fig. 2. Illustration of deformable audio Transformer.

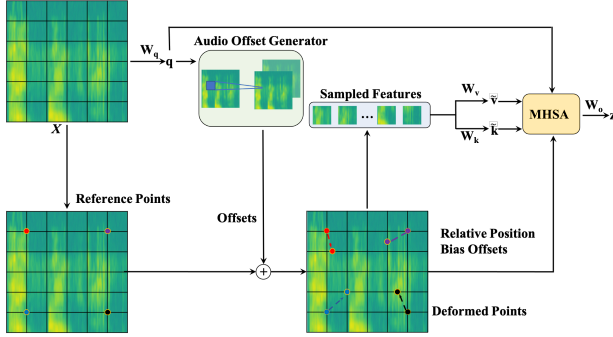


Fig. 3. Illustration of spectrogram deforming processing. Audio offset generator in §3.1 calculates offsets used in deformable attention. When applying the deformable attention on the audio spectrum, for each query token, we select the most informative spectrum patch to conduct the self-attention. Based on the query location, DATAR learns the offset to localize the target spectrum patches.

$\{(0, 0), \dots, (h_G - 1, T_G - 1)\}$. Then we normalize them to the range $[-1, 1]$ according to the grid shape $h_G \times T_G$, in which $(-1, -1)$ indicates the top-left corner and $(1, 1)$ indicates the bottom-right corner.

Without loss of generality, we still use X as input for each block and omit the patch embedding and reshaping operators. To obtain the offset for each reference point, the feature maps are projected linearly to the query tokens $q = XW_q$, and then fed into a lightweight subnetwork $\theta_{\text{offset}}(\cdot)$ to generate the offsets $\Delta p = \theta_{\text{offset}}(q)$. To stabilize the training process, we scale the amplitude of Δp by a predefined factor s to prevent too large offset, *i.e.*, $\Delta p \leftarrow s \tanh(\Delta p)$. Then the features are sampled at the locations of deformed points as keys and values, followed by projection matrices:

$$q = XW_q, \quad \tilde{k} = \tilde{X}W_k, \quad \tilde{v} = \tilde{X}W_v, \\ \text{with } \Delta p = \theta_{\text{offset}}(q), \quad \tilde{X} = \phi(X; p + \Delta p), \quad (2)$$

where \tilde{k} and \tilde{v} represent the deformed key and value embeddings respectively. Specifically, we set the sampling function

$\phi(\cdot; \cdot)$ to a bilinear interpolation to make it differentiable:

$$\phi(z; (p_x, p_y)) = \sum_{(r_x, r_y)} g(p_x, r_x)g(p_y, r_y)z[r_y, r_x, :], \quad (3)$$

where $g(a, b) = \max(0, 1 - |a - b|)$ and (r_x, r_y) indexes all the locations on $z \in \mathbb{R}^{h \times T \times C}$. As g would be non-zero only on the four integral points closest to (p_x, p_y) , it simplifies Eq. (3) to a weighted average of the four locations. We perform multi-head attention on q, \tilde{k}, \tilde{v} and adopt relative position offsets R . The output of an attention head is formulated as:

$$z^{(m)} = \sigma \left(q^{(m)} \tilde{k}^{(m)\top} / \sqrt{d} + \phi(\hat{B}; R) \right) \tilde{v}^{(m)}, \quad (4)$$

where $\phi(\hat{B}; R) \in \mathbb{R}^{hT \times hGT_G}$ corresponds to the position embedding following previous work [7].

Audio offset generator A subnetwork is adopted for offset generation, which consumes the query features and outputs the offset values for reference points. Considering that each reference point covers a local $s \times s$ region where s is the largest value for offset, the generation network should also have the perception of the local features to learn reasonable offsets. Therefore, we implement the subnetwork as two convolution modules with a nonlinear activation in Fig. 3. The input features are first passed through a 5×5 depth-wise convolution to capture local features. Then, a GELU activation and a 1×1 convolution is adopted to get the 2D offsets. It is also worth noticing that the bias in 1×1 convolution is dropped to alleviate the compulsive shift for all locations.

Deformable relative position bias Relative position bias encodes the relative positions between every pair of query and key, which augments the vanilla attention with spatial information. Considering a feature map with shape $h \times T$, its relative coordinate displacements lie in the range of $[-h, h]$ and $[-T, T]$ at two dimensions, respectively. In Swin Transformer [7], a relative position bias table $\hat{B} \in \mathbb{R}^{(2h-1) \times (2T-1)}$ is constructed to obtain the relative position bias by indexing the table with the relative displacements in two directions. Since our deformable attention has continuous positions of keys, we compute the relative displacements in the normalized range $[-1, 1]$, and then interpolate $\phi(\hat{B}; R)$ in the parameterized bias table $\hat{B} \in \mathbb{R}^{(2h-1) \times (2T-1)}$ by the continuous relative displacements in order to cover all possible offset values.

3.2. Learnable Input Adaptor

To further increase the accuracy, we apply a 2D convolution over an input signal composed of several input planes. In the simplest case, the output value of the layer with input size (C, h, T) and output can be defined as:

$$\text{out}(C_j) = \text{input}(C_j) + \lambda(\text{b}(C_j) + \sum_{k=0}^{C-1} \text{W}(C_j, k) * \text{input}(k)), \quad (5)$$

where C_j is the channel index, λ is used to tune the strength of adaptor, b and W are learnable parameters to enhance input signals, $*$ is a 2D cross-correlation operator, C denotes the number of channels, h is the number of triangular mel-frequency bins, and T is the temporal length, $\text{input}(k)$ denotes the k -th channel of input.

4. EXPERIMENTS

We experiment with three audio event classification datasets – Kinetics-Sounds [38, 39], Epic-Kitchens-100 [40, 41, 42], and VGGSound [43]. The input is TorchAudio-based fbank, which is a log-compressed mel-scaled spectrogram and the same as AST. The frame length is 1,024 and the number of triangular mel-frequency bins is 128, which are the same as AST. The sampling frequency is 43,000 to cover 10 seconds of audio. We use cross-entropy loss. On Epic-Kitchens-100, we employ two classification heads for verb and noun.

Kinetics-Sounds [39, 38] is a commonly used subset of the Kinetics-400 dataset [39], which is composed of 10-second audio data from YouTube. The dataset collection protocol described in [44] is followed. 22,914 valid training audio data and 1,585 valid test audio data are collected. Epic-Kitchens-100 [42] consists of 90,000 variable length egocentric clips spanning 100 hours capturing daily kitchen activities. The dataset formulates each action into a verb and a noun. There are 67,217 training and 9,668 test samples after we remove categories with no training sample, which results in 97 verbs and 293 nouns. VGGSound [43] consists of about 200,000 10-second video clips and 309 categories ranging from human actions and sound-emitting objects to human-object interactions. After removing invalid audio data, 159,223 valid training audio data and 12,790 valid test audio data are collected. **Hyperparameters** In all the experiments, we follow AST [21] setting in which model is pre-trained on ImageNet-1k. For hyperparameters in DATAR, we follow DAT [12] and use ImageNet-1K publicly available pretrained weights. AdamW is used with the learning rate of 0.00001. The numbers of epochs are set as 300, 100, and 50 for Kinetics-Sounds, Epic-Kitchens-100, and VGGSound. We employ the code of AST to obtain the results on these datasets.

Comparison with state-of-the-arts According to Table 1, 2, and 3, the comparative results show that the proposed method is effective, and it outperforms the previous state-of-the-arts by a large margin. Specifically, the DATAR outperforms the previous best methods by 18.9%, 3.2% and 0.9% in terms of top-1 accuracy on the three datasets. The main reason is that, the introduced deformable audio attention and the learnable input adaptor help the model effectively capture the informative audio signals which are used to boost the model performance. For computation complexity, our work achieves better accuracy and consumes 93.3G MACs, while AST uses 103.4G MACs on VGGSound.

Ablation study To validate the effectiveness of the proposed

| Model | Top-1 acc | Top-5 acc |
|----------------------------|-------------|-------------|
| AST [45] | 52.6 | 71.5 |
| DATAR (deformable+adaptor) | 71.5 | 90.5 |

Table 1. Comparison with state-of-the-arts on Kinetics-Sounds.

| Model | Top-1 acc | Top-5 acc |
|----------------------------|-------------|-------------|
| AST [45] | 52.3 | 78.1 |
| Chen et al. [43] | 48.8 | 76.5 |
| AudioSlowFast [4] | 50.1 | 77.9 |
| DATAR (deformable+adaptor) | 55.5 | 80.2 |

Table 2. Comparison with state-of-the-arts on VGGSound.

| Model | Verb | Noun | Action |
|----------------------------|-------------|-------------|-------------|
| AST [45] | 44.3 | 22.4 | 13.0 |
| Damen et al. [40] | 42.1 | 21.5 | 14.8 |
| AudioSlowFast [4] | 46.5 | 22.8 | 15.4 |
| DATAR (deformable+adaptor) | 48.7 | 22.9 | 16.3 |

Table 3. Comparison with state-of-the-arts on Epic-100.

| Model | Top-1 | Top-5 |
|--------------------------------------|-------------|-------------|
| without deformable | 69.4 | 86.6 |
| with deformable | 70.5 | 89.9 |
| deformable + $\mathcal{N}(0, 0.005)$ | 70.2 | 90.1 |
| deformable + $\mathcal{L}(0, 0.005)$ | 70.5 | 89.6 |
| deform.+adaptor: $\lambda = 0.2$ | 70.5 | 90.2 |
| deform.+adaptor: $\lambda = 0.005$ | 71.5 | 90.5 |

Table 4. Ablation study on Kinetics-Sounds.

deformable audio attention and the input adaptor, we conduct the ablation study of ‘without deformable’, ‘with deformable’, adding Gaussian perturbation to the input instead of learnable adaptor, adding Laplacian perturbation, different strengths, 0.2, 0.005, of λ in Table 4. Deformable audio attention helps improve the model performance, *i.e.*, 1.1% improvement in terms of top-1 accuracy on Kinetics-Sounds dataset. Based on Table 4, the proposed input adaptor is effective and improves the baseline model (DATAR with deformable) by 1% in top-1 accuracy. Compared with Gaussian and Laplacian perturbations, the proposed DATAR with the learnable input adaptor surpasses the two perturbation based methods by 1.3% and 1%. This demonstrates the effectiveness of learnable input adaptor.

5. CONCLUSION

We propose a novel deformable audio transformer for audio event classification, DATAR, which consists of deformable audio attention and input adaptor. Moreover, a learnable input adaptor is introduced to alleviate the issue of over-simplifying the input feature of deformable attention. Extensive results demonstrate the effectiveness of the proposed approach.

6. REFERENCES

- [1] Ashish Vaswani et al., “Attention is all you need,” in *NeurIPS*, 2017, vol. 30.
- [2] Anmol Gulati et al., “Conformer: Convolution-augmented transformer for speech recognition,” in *Proc. Interspeech*, 2020.
- [3] Qiuqiang Kong et al., “Sound event detection of weakly labelled data with cnn-transformer and automatic threshold optimization,” *IEEE/ACM TASLP*, vol. 28, pp. 2450–2460, 2020.
- [4] Evangelos Kazakos et al., “Slow-fast auditory streams for audio recognition,” in *ICASSP*. IEEE, 2021.
- [5] Manzil Zaheer et al., “Big bird: Transformers for longer sequences,” in *NeurIPS*, 2020, vol. 33, pp. 17283–17297.
- [6] Iz Beltagy et al., “Longformer: The long-document transformer,” *arXiv preprint arXiv:2004.05150*, 2020.
- [7] Ze Liu et al., “Swin transformer: Hierarchical vision transformer using shifted windows,” in *Proceedings of ICCV*, 2021.
- [8] Wenhai Wang et al., “Pyramid vision transformer: A versatile backbone for dense prediction without convolutions,” in *Proceedings of ICCV*, 2021, pp. 568–578.
- [9] Jifeng Dai et al., “Deformable convolutional networks,” in *Proceedings of ICCV*, 2017, pp. 764–773.
- [10] Xizhou Zhu et al., “Deformable DETR: Deformable Transformers for End-to-End Object Detection,” in *ICLR*, 2021.
- [11] Jue Wang and Lorenzo Torresani, “Deformable video transformer,” in *Proceedings of CVPR*, 2022, pp. 14053–14062.
- [12] Zhuofan Xia et al., “Vision transformer with deformable attention,” in *Proceedings of CVPR*, 2022.
- [13] Yue Cao et al., “GCNet: Non-local networks meet squeeze-excitation networks and beyond,” in *Proceedings of ICCV Workshop*, 2019.
- [14] Daquan Zhou et al., “DeepViT: Towards deeper vision transformer,” *arXiv preprint arXiv:2103.11886*, 2021.
- [15] Yuan Gong, Yu-An Chung, and James Glass, “AST: Audio spectrogram transformer,” in *Interspeech*, 2021.
- [16] Ke Chen et al., “HTS-AT: A hierarchical token-semantic audio transformer for sound classification and detection,” in *ICASSP*. IEEE, 2022, pp. 646–650.
- [17] Wentao Zhu and Mohamed Omar, “Multiscale audio spectrogram transformer for efficient audio classification,” in *ICASSP 2023-2023 IEEE International Conference on Acoustics, Speech and Signal Processing (ICASSP)*. IEEE, 2023, pp. 1–5.
- [18] Wentao Zhu, “Efficient multiscale multimodal bottleneck transformer for audio-video classifications,” 2024.
- [19] Wentao Zhu, “Efficient selective audio masked multimodal bottleneck transformer for audio-video classification,” 2024.
- [20] Koichi Miyazaki et al., “Convolution augmented transformer for semi-supervised sound event detection,” in *DCASE*, 2020.
- [21] Qiuqiang Kong et al., “PANNS: Large-scale pretrained audio neural networks for audio pattern recognition,” *IEEE/ACM TASLP*, vol. 28, pp. 2880–2894, 2020.
- [22] Yuan Gong, Yu-An Chung, and James Glass, “PSLA: Improving audio tagging with pretraining, sampling, labeling, and aggregation,” *IEEE/ACM TASLP*, vol. 29, pp. 3292–3306, 2021.
- [23] Oleg Rybakov et al., “Streaming keyword spotting on mobile devices,” in *Proc. Interspeech*, 2020, pp. 2277–2281.
- [24] Alexey Dosovitskiy et al., “An image is worth 16x16 words: Transformers for image recognition at scale,” in *International Conference on Learning Representations*, 2021.
- [25] Chun-Fu Chen et al., “RegionViT: Regional-to-Local Attention for Vision Transformers,” in *ICLR*, 2022.
- [26] Xiaoyi Dong et al., “CSWin transformer: A general vision transformer backbone with cross-shaped windows,” in *CVPR*, 2022, pp. 12124–12134.
- [27] Xuran Pan et al., “On the integration of self-attention and convolution,” in *CVPR*, 2022, pp. 815–825.
- [28] Jianwei Yang et al., “Focal self-attention for local-global interactions in vision transformers,” *arXiv preprint arXiv:2107.00641*, 2021.
- [29] Pengchuan Zhang et al., “Multi-scale vision longformer: A new vision transformer for high-resolution image encoding,” in *ICCV*, 2021, pp. 2998–3008.
- [30] Andrew Jaegle et al., “Perceiver: General perception with iterative attention,” in *ICML*. PMLR, 2021, pp. 4651–4664.
- [31] Song Bai et al., “Visual parser: Representing part-whole hierarchies with transformers,” *arXiv preprint arXiv:2107.05790*, 2021.
- [32] Yulin Wang et al., “Not all images are worth 16x16 words: Dynamic transformers for efficient image recognition,” *NeurIPS*, vol. 34, pp. 11960–11973, 2021.
- [33] Xizhou Zhu et al., “Deformable ConvNets v2: More deformable, better results,” in *CVPR*, 2019, pp. 9308–9316.
- [34] Xiaoyu Yue et al., “Vision transformer with progressive sampling,” in *ICCV*, 2021, pp. 387–396.
- [35] Zhiyang Chen, Yousong Zhu, Chaoyang Zhao, Guosheng Hu, Wei Zeng, Jinqiao Wang, and Ming Tang, “Dpt: Deformable patch-based transformer for visual recognition,” in *Proceedings of the 29th ACM International Conference on Multimedia*, 2021, pp. 2899–2907.
- [36] Nicolas Carion, Francisco Massa, Gabriel Synnaeve, Nicolas Usunier, Alexander Kirillov, and Sergey Zagoruyko, “End-to-end object detection with transformers,” in *European Conference on Computer Vision*. Springer, 2020, pp. 213–229.
- [37] Jimmy Lei Ba, Jamie Ryan Kiros, and Geoffrey E Hinton, “Layer normalization,” *arXiv preprint arXiv:1607.06450*, 2016.
- [38] Relja Arandjelovic and Andrew Zisserman, “Look, listen and learn,” in *Proceedings of ICCV*, 2017, pp. 609–617.

- [39] Will Kay et al., “The kinetics human action video dataset,” *arXiv preprint arXiv:1705.06950*, 2017.
- [40] Dima Damen et al., “Rescaling Egocentric Vision: Collection, Pipeline and Challenges for EPIC-KITCHENS-100,” *IJCV*, 2021.
- [41] Dima Damen, Hazel Doughty, et al., “Scaling egocentric vision: The EPIC-KITCHENS dataset,” in *ECCV*, 2018, pp. 720–736.
- [42] Dima Damen et al., “The EPIC-KITCHENS Dataset: Collection, Challenges and Baselines,” *IEEE TPAMI*, 2021.
- [43] Honglie Chen, Weidi Xie, Andrea Vedaldi, and Andrew Zisserman, “VGGSound: A large-scale audio-visual dataset,” in *ICASSP*. IEEE, 2020.
- [44] Fanyi Xiao, Yong Jae Lee, Kristen Grauman, Jitendra Malik, and Christoph Feichtenhofer, “Audiovisual slowfast networks for video recognition,” *arXiv preprint arXiv:2001.08740*, 2020.
- [45] Arsha Nagrani et al., “Attention bottlenecks for multimodal fusion,” in *NeurIPS*, 2021.